Intercalates of Bi_2Se_3 Studied *in Situ* by Time-Resolved Powder X-ray Diffraction and Neutron Diffraction

Machteld E. Kamminga, Simon J. Cassidy, Partha P. Jana,[a] Nicola D. Kelly,[b] Simon J. Clarke[*]

Department of Chemistry, University of Oxford, Inorganic Chemistry Laboratory, South Parks Road, Oxford OX1 3QR, United Kingdom.

[a] Current address: *Department of Chemistry, IIT Kharagpur, India-721302.*

[b] Current address: *Cavendish Laboratory, Department of Physics, University of Cambridge, JJ Thomson Avenue, Cambridge CB3 0HE, United Kingdom.*

[*] E-mail: simon.clarke@chem.ox.ac.uk

Intercalation of lithium and ammonia into the layered semiconductor Bi_2Se_3 proceeds via a hyperextended (by > 60 %) ammonia-rich intercalate, to eventually produce a layered compound with lithium amide intercalated between the bismuth selenide layers which offer scope for further chemical manipulation.

Bismuth selenide, Bi_2Se_3, is of contemporary interest as a thermoelectric material,[1–5] and as a layered topological insulator.[6] The structure consists of quintuple Se-Bi-Se-Bi-Se layers separated by a van der Waals gap and invites the intercalation chemistry well known in layered chalcogenides.[7–9] Direct intercalation of zerovalent metals such as Cu into the structure results in complex superstructures;[10] high temperature reactions of elemental reagents yield Bi_2Se_3 derivatives containing Cu, Sr and Nb which exhibit superconductivity.[11–13] These are often described as intercalates with the assumption that the additional metal occupies the interlayer space, although many of these are not well characterised with respect to either composition or crystal structure. Co-intercalation of alkali metals and ammonia/amide has shown to produce dramatic changes in physical properties, *e.g.* in the case of the superconductor FeSe.[14,15] Here we probe the reaction between Li/ammonia and Bi_2Se_3 to produce two products with different ammonia contents that invite further investigations and expand the scope of this chemistry.

Fig. 1(a) shows portions of the synchrotron X-ray diffractograms showing the evolution of the lowest angle 003 peak of Bi_2Se_3 and the final intercalated $Li_x(NH_2/NH_3)_yBi_2Se_3$ product obtained in reactions with varying Li:Bi_2Se_3 compositions ($0.2 \leq x \leq 1.0$). A large shift in the lowest angle peak to still lower angles is observed, indicating a large increase in the separation of the quintuple layers upon intercalating Li and ammonia into the van der Waals gap of Bi_2Se_3. As a control, it was checked that suspending Bi_2Se_3 in liquid ammonia without any Li did not result in any changes in the diffraction pattern. For small amounts of Li (x = 0.2 and 0.3) not all the Bi_2Se_3 is consumed, but a new reflection emerges at 2θ ~4.5° (*i.e.* d ~10.5 Å). Upon increasing x to 0.4, no crystalline Bi_2Se_3 remains and a very broad peak is observed with a centre of gravity at 2θ ~3.9° (*i.e.* d ~12 Å). Addition of up to one mole of Li per mole of Bi_2Se_3 leads a single phase product with a narrow 003 peak at 2θ ~3.65° (*i.e.* d ~12.9 Å). Rietveld refinements of Bi_2Se_3 and $Li_x(NH_2/NH_3)_yBi_2Se_3$ with x = 1.0 are shown in Fig. S1 in the

supporting information. Note that the peak shapes for the intercalated phase are broader than in the parent Bi_2Se_3 with the profile parameters suggesting strain-related broadening. The very broad peaks for $x < 1$ suggest stacking disorder, possibly as a consequence of staging which requires further analysis.

X-ray diffraction intensities are dominated by the contributions from Bi and Se, so powder neutron diffraction (PND) measurements on the crystalline intercalates obtained by reacting Li with Bi_2Se_3 in a ratio of 1:1 were conducted. Samples of both $Li_x(NH_2/NH_3)_yBi_2Se_3$ and $Li_x(ND_2/ND_3)_yBi_2Se_3$ were measured at 5K and room temperature to attempt to constrain the refined models with the expectation of some disorder in the intercalates. H and D have very different neutron scattering lengths (-3.7406 fm for H and +6.671 fm for D), H is a strong incoherent scatterer, and H and Li both have negative scattering lengths. Selected diffraction patterns and Rietveld refinements are given in Fig. 2 and Fig. S2 in the supporting information. A single structural model was refined against all four datasets as explained further in the supporting information. Structural and refinement parameters are listed in Table S1 in the supporting information.

A positive scattering centre located at (1/3, 2/3, 0.50020(6)) – a trigonal prismatic site formed by Se atoms of adjacent Bi_2Se_3 layers – corresponded to an occupancy of 0.44(1) N. There was no sign of a net negative scattering centre corresponding to Li. Taking the different scattering lengths into account (+9.36 fm for N and -1.90 fm for Li), the scattering centre at (1/3, 2/3, 0.50020(6)) corresponds to ~0.53(1) N and ~0.47(1) Li, suggesting disorder of Li and NH_2/NH_3 moieties on the length scale probed by diffraction and with $x = y = 1$ in the formula $Li_x(NH_3/NH_2)_yBi_2Se_3$, consistent with the $Li:Bi_2Se_3$ ratio in the synthesis. A realistic structural model for a single intercalate layer (Fig. S3 in the supporting information), has each NH_x moiety surrounded strictly by three Li (and vice versa) at ~2.4 Å comparable to the Li-N bond length of ~2.0-2.2 Å in crystalline $LiNH_2$.[16] In our model these intercalate layers are disordered along the *c*-direction, hence the average scatting at the (1/3, 2/3, 0.50020(6)) site corresponds to the Li/N disorder on the length scale probed by the diffraction experiment. The H and D atoms were located approximately 1 Å from the N atoms, while applying a soft restraint for the N-H/D distance, and this results in weak N-H···Se hydrogen bonds of ~2.8 Å (H···Se distance), similar to ammonia intercalates of FeSe[14] and TiS_2.[17] In this model the amide moieties

are orientationally disordered on the length scale of the diffraction experiment. No further scattering density corresponding to further NH_2 or NH_3 moieties could be located. The refinement produced an H (or D) to N ratio of 2.10(2), so within the experimental uncertainty the intercalate layer is neutral lithium amide and the overall formula is $LiNH_2Bi_2Se_3$. Consistent with this, SQUID magnetometry (Fig. S4 in the supporting information) shows a minimal change in the overall diamagnetic susceptibility (from $-3.19(6) \times 10^{-4}$ to $-2.72(9) \times 10^{-4}$) with no evidence for a substantial injection of electrons into the conduction band to produce a Pauli paramagnetic susceptibility to oppose the diamagnetism of the core electrons. This is consistent with the difficulty of partially reducing Bi^{3+}. Conductivity measurements were hampered by the air sensitivity and thermal sensitivity (see below) of these finely divided powders.

To probe the course of the intercalation reaction, we performed the reaction *in situ* at the I12 beamline at the Diamond Light Source (see the supporting information for details). Fig. 3(a) shows the diffraction patterns measured at four different time stamps. The red pattern shows the background (see the supporting information). The blue pattern (t = 0 s) shows the synchrotron PXRD (powder X-ray diffraction) pattern directly after tipping the Bi_2Se_3 into the Li/NH_3 solution, which corresponds to pure Bi_2Se_3, (Fig. 6(a) in the supporting information). The characteristic first peak with a *d*-spacing of 9.483(2) Å (003 reflection in the hexagonal setting of space group *R*-3*m*) corresponds to the separation between adjacent Bi_2Se_3 quintuple layers. After about two minutes, a second set of diffraction peaks appears, with the first reflection at 15.380(3) Å, indicating that the interlayer distance has increased by a remarkable 62 % upon intercalation. Figs. 3(b,c) show the detailed time lapse of the intercalation.

The product obtained in this *in situ* experiment is measured while suspended in liquid ammonia and has a much larger interlayer separation than the dry product described above using PND. After boiling off the ammonia and evacuating the reaction vessel to produce a dry product as in the lab experiment, the first peak shifts to 12.83(1) Å corresponding to the lab-synthesised product described in detail above with an interlayer distance 35 % larger than in Bi_2Se_3. Note that evacuation is necessary to fully develop the ammonia-poor compound (see Table 1). The highly expanded phase can be regained by suspending the dry evacuated product in liquid ammonia shown in Fig. 3(d) and Fig. S5 in the supporting information, suggesting that the new

phase identified in the *in situ* measurement is an ammonia rich phase. Fig. 3(d) shows that evacuation is required to fully remove all the NH_3 molecules from the intercalate to result in the product $LiNH_2Bi_2Se_3$. We note that suspending the evacuated product in liquid ammonia gives rise to a re-ammoniated product with a very slightly different d_{003}-spacing to that measured *in situ* (by less than 1%). Because the sample was removed from the diffractometer and placed back into the beam between each step in Fig. 3(d), we cannot rule out that this small difference is an artefact of the experiment, although the two ammonia-rich phases were obtained by different routes, and may differ slightly in their level of intercalated ammonia.

The superconducting Li/NH_3 intercalates of FeSe also show ammonia-rich and ammonia-poor phases. In that case the ammonia-rich phase could be stabilised in dry form by exposing it to 1 bar of ammonia gas at -20 °C.[15] The ammonia-rich intercalated phase of Bi_2Se_3 could not be regenerated in the dry form, hampering analysis by PND. The I12 synchrotron data (Rietveld refinements shown in Fig. S6 in the supporting information) together with sensible assumptions about bond lengths was used to propose a model for the crystal structure as shown in Fig. 4(b). Fig. S7 in the supporting information shows that adding one mole of ammonia per mole of $LiNH_2Bi_2Se_3$ results in a tetrahedral coordination of N around Li with sensible interatomic distances: the Li-NH_2 distance is ~2.5 Å and the N-H···Se hydrogen bonds have H···Se ~2.9 Å, indicating weak hydrogen bonds, which is consistent with the distance found in other intercalates.[14,17]

Based on the abovementioned model for the intercalated end product as determined by neutron diffraction, we extended the model to incorporate our suggested intermediate phase to: $LiNH_2(NH_3)_zBi_2Se_3$, where $z \leq 1$ NH_3 can be added or removed by changing between the final and intermediate phase (see Fig. 4). The lattice parameters are given in Table 1.

In Bi_2Se_3 the quintuple layers are stacked in an *ABCABC*-type fashion, resulting in the rhombohedral symmetry. Upon intercalation to form the intermediate, ammonia-rich phase, this stacking is maintained. Upon drying, with the loss of the ammonia to form $LiNH_2Bi_2Se_3$, a rearrangement of the layers occurs resulting in an *ACBACB*-type fashion. This maintains rhombohedral symmetry, but has a different relative arrangement of the layers (Fig. 4(c)) with

the layers of selenide ions coordinated to the intercalated species eclipsed when viewed along the *c* direction, while in Bi_2Se_3 and in the ammonia-rich intercalate phase they are staggered (Figs. 4(a-b)). These changes are presumably driven by the coordination requirements of the intercalated molecules, and these changes mimic those that are found in the Li/NH_3 intercalates of FeSe.[14,15]

$LiNH_2Bi_2Se_3$ decomposes on heating above 450 K. As shown in Fig. S8, in the supporting information, between 480 and 490 K there is a broadening of the lowest angle reflection, together with a dramatic shift with a new, fairly crystalline phase formed at 490 K which has the first reflection equated with the interlayer separation at ~11.8 Å, smaller than in the intercalate phases, but much larger than in Bi_2Se_3. The relatively broad diffraction peaks of this phase hampered further structural characterisation, but it suggests further complexity in the intercalated Bi_2Se_3 phase field. Heating above 495 K resulted in further decomposition.

These results show that in intercalates of layered compounds with metal ions and small molecules the adoption of both molecule-rich and molecule-poor structures is not uncommon. These intercalates do not show desirable properties such as the superconductivity reportedly induced in other derivatives of Bi_2Se_3, but they offer a starting point for further compositional tuning to tune electronic properties, and chemical routes to new materials via exfoliation and ion exchange. Further investigations of Li and H/D mobilities and the range of compositions available in the ammonia-rich and ammonia-poor phase fields is in progress.

Acknowledgements

MEK was supported by the Netherlands Organisation for Scientific Research (NWO, grant code 019.181EN.003). PPJ was supported by the EU Horizon 2020 MSCA Individual Fellowship 658832 (SOLLAY). We thank EPSRC (EP/R042594, EP/P018874, EP/M020517), DLS Ltd for beam time (EE18786/EE20375), Dr Clare Murray for assistance on I11, Dr Stefan Michalik for assistance on I12, ISIS for beam time (RB1720128/RB190122) and Dr Ron Smith for assistance at POLARIS.

Competing interests

The authors declare no competing interests.

Additional information

Supporting information is available for this paper at the end of this document.

Correspondence and requests for materials should be addressed to S.J.**C.**

Notes and references

1 R. Liu, X. Tan, G. Ren, Y. Liu, Z. Zhou, C. Liu, Y. Lin and C. Nan, *Crystals*, 2017, **7**, 257.

2 Y. S. Hor, A. Richardella, P. Roushan, Y. Xia, J. G. Checkelsky, A. Yazdani, M. Z. Hasan, N. P. Ong and R. J. Cava, *Phys. Rev. B*, 2009, **79**, 195208.

3 A. Al Bayaz, A. Giani, A. Foucaran, F. Pascal-Delannoy and A. Boyer, *Thin Solid Films*, 2003, **441**, 1–5.

4 D. Kim, P. Syers, N. P. Butch, J. Paglione and M. S. Fuhrer, *Nano Lett.*, 2014, **14**, 1701–1706.

5 G. Sun, X. Qin, D. Li, J. Zhang, B. Ren, T. Zou, H. Xin, S. Buehler Paschen and X. Yan, *J. Alloy. Compd.*, 2015, **639**, 9–14.

6 H. Zhang, C.-X. Liu, X.-L. Qi, X. Dai, Z. Fang and S.-C. Zhang, *Nat. Phys.*, 2009, **5**, 438–442.

7 H. Yuan, H. Wang and Y. Cui, *Acc. Chem. Res.*, 2015, **48**, 81–90.

8 Y. Jung, Y. Zhou and J. J. Cha, *Inorg. Chem. Front.*, 2016, **3**, 452–463.

9 J. Buha and L. Manna, *Chem. Mater.*, 2017, **29**, 1419–1429.

10 K. J. Koski, C. D. Wessells, B. W. Reed, J. J. Cha, D. Kong and Y. Cui, *J. Am. Chem. Soc.*, 2012, **134**, 13773–13779.

11 Y. S. Hor, J. G. Checkelsky, D. Qu, N. P. Ong and R. J. Cava, *J. Phys. Chem. Solids*, 2011, **72**, 572–576.

12 Y. S. Hor, A. J. Williams, J. G. Checkelsky, P. Roushan, J. Seo, Q. Xu, H. W. Zandbergen, A. Yazdani, N. P. Ong and R. J. Cava, *Phys. Rev. Lett.*, 2010, **104**, 057001.

13 Shruti, V. K. Maurya, P. Neha, P. Srivastava and S. Patnaik, *Phys. Rev. B*, 2015, **92**, 020506.

14 M. Burrard-Lucas, D. G. Free, S. J. Sedlmaier, J. D. Wright, S. J. Cassidy, Y. Hara, A. J. Corkett, T. Lancaster, P. J. Baker, S. J. Blundell and S. J. Clarke, *Nat. Mater.*, 2013, **12**, 15–19.

15 S. J. Sedlmaier, S. J. Cassidy, R. G. Morris, M. Drakopoulos, C. Reinhard, S. J. Moorhouse, D. O'Hare, P. Manuel, D. Khalyavin and S. J. Clarke, *J. Am. Chem. Soc.*, 2014, **136**, 630–633.

16 J. B. Yang, X. D. Zhou, Q. Cai, W. J. James and W. B. Yelon, *Appl. Phys. Lett.*, 2006, **88**, 041914.

17 V. G. Young, M. J. McKelvy, W. S. Glaunsinger and R. B. Von Dreele, *Chem. Mater.*, 1990, **2**, 75–81.

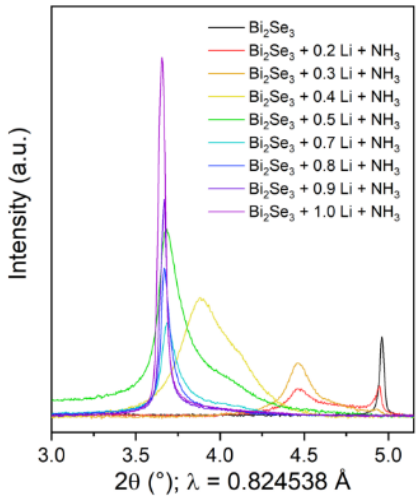

Fig. 1 The lowest angle 003 peak of Bi_2Se_3 and $Li_x(NH_2/NH_3)_yBi_2Se_3$ with varying targeted Li content ($0.2 \leq x \leq 1.0$).

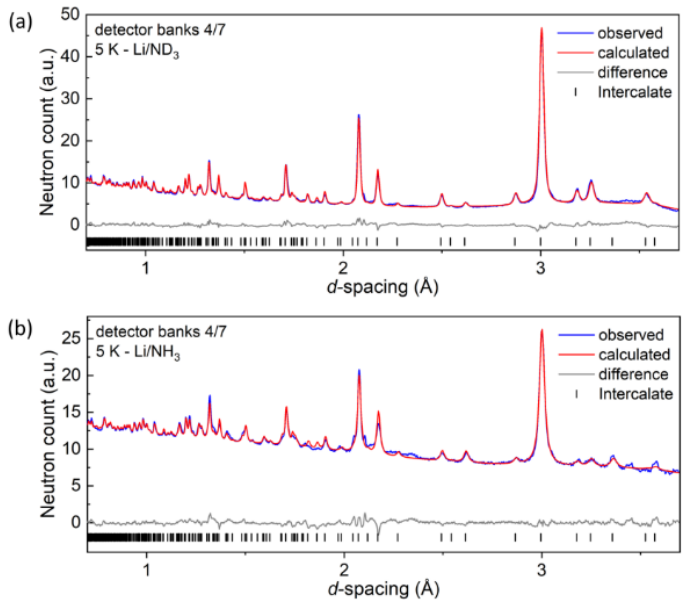

Fig. 2. Rietveld refinements of the structure of the (a) Li/ND_3 and (b) Li/NH_3 intercalates against POLARIS data at 5 K. Peak positions are marked by vertical lines.

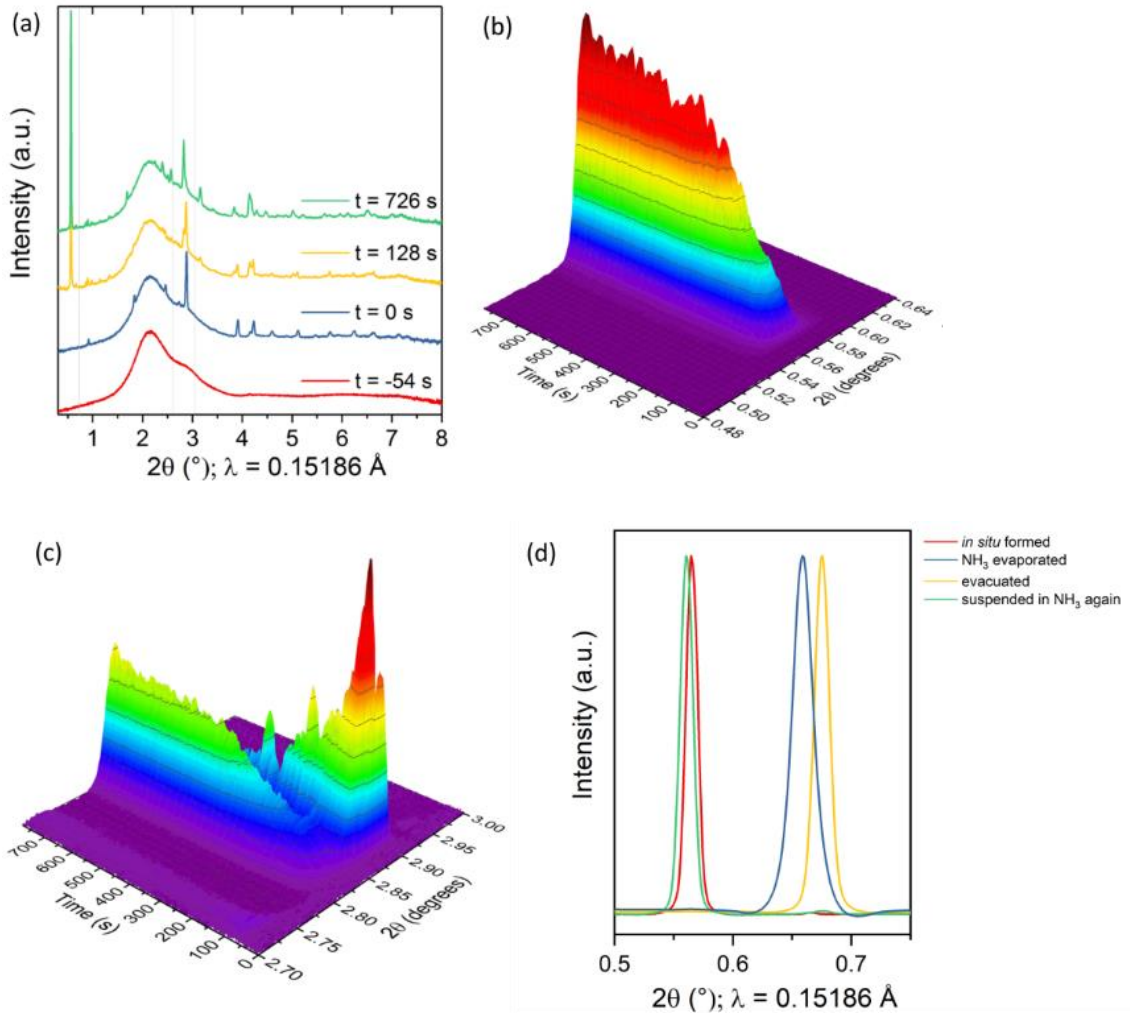

Fig. 3. (a) Diffraction patterns from integration of the Bragg rings measured on I12 at four different moments during the *in situ* reaction. The patterns are off-set for clarity. The background from the glass and liquid was treated as described in the supporting information. The dotted lines indicate the ranges plotted in (b) and (c). Time lapse of the *in situ* PXRD measurement showing (b) the rise of the 003 peak of the intercalate phase and (c) the simultaneous decrease of the 015 peak of the parent compound and the rise of the 018 peak of the intercalate phase over time. (d) 003 peak of the ammonia-rich intercalate as formed during the *in situ* reaction, after evaporation of NH_3, after evacuation, and after suspending again in liquid ammonia, showing the reversible nature of ammonia desorption as shown in Fig. 4. The background is subtracted for clarity.

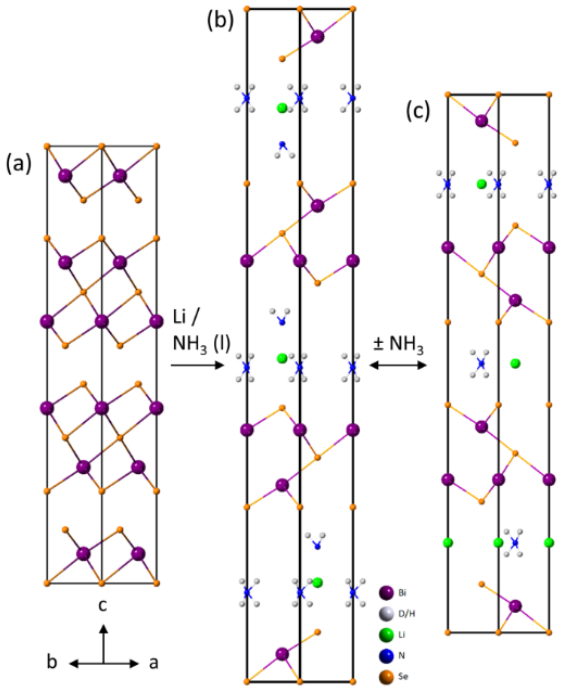

Fig. 4 Schematic of crystal structures of (a) Bi_2Se_3, (b) the intercalation of lithium and ammonia into Bi_2Se_3 to form the ammonia-rich intercalate, and (c) the reversible ammonia desorption of the intercalated Bi_2Se_3. Note that in (b) and (c), Li and N actually occupy the same site, resulting in a disordered structure. Here, a possible arrangement is given for clarity.

Table 1. Lattice parameters and cell volumes of Bi_2Se_3 and intercalates, determined from I12 PXRD data. The colour coding corresponds to Fig. 3(d) and the bold-faced data corresponds to the structures drawn in Fig. 4.

	a (Å)	*c* (Å)	*V* (Å^3)	d_{003}-spacing = *c*/3 (Å)
Bi_2Se_3	**4.1157(4)**	**28.449(4)**	**417.3(1)**	**9.483(2)**
● **ammonia rich intercalate**	**4.1852(3)**	**46.140(7)**	**699.91(14)**	**15.380(3)**
● Evaporated intercalate	4.1928(9)	39.68(3)	604.1(5)	13.23(1)
● **Evacuated intercalate**	**4.1780(11)**	**38.49(3)**	**581.88(5)**	**12.83(1)**
● suspended again intercalate	4.1634(4)	46.467(11)	697.54(19)	15.489(4)

Supporting information for

Intercalates of Bi_2Se_3 Studied *in Situ* by Time-Resolved Powder X-ray Diffraction and Neutron Diffraction

Machteld E. Kamminga, Simon J. Cassidy, Partha P. Jana,[a] Nicola D. Kelly,[b] Simon J. Clarke[*]

Department of Chemistry, University of Oxford, Inorganic Chemistry Laboratory, South Parks Road, Oxford OX1 3QR, United Kingdom.

[a] Current address: *Department of Chemistry, IIT Kharagpur, India-721302.*

[b] Current address: *Cavendish Laboratory, Department of Physics, University of Cambridge, JJ Thomson Avenue, Cambridge CB3 0HE, United Kingdom.*

[*] E-mail: simon.clarke@chem.ox.ac.uk

Experimental Section

Synthesis

All manipulations were carried out in a Glovebox Technology argon-filled dry box with an O_2 and H_2O content below 1 ppm or on a Schlenk line. The parent compound Bi_2Se_3 was synthesized by mixing together high-purity Bi pieces (Sigma Aldrich; 99.999%) and Se powder (Alfa Aeser; 99.999%) and heating them in a sealed silica tube to 720 °C at 2 °C min^{-1}, holding the temperature for 48 h, cooling to room temperature at the natural rate of the furnace, grinding the product into a fine powder and repeating the heating procedure with the same ramp rate and holding at 720 °C for 72 h before cooling to room temperature.

The intercalates, $Li_x(NH_2/NH_3)_yBi_2Se_3$ and $Li_x(ND_2/ND_3)_yBi_2Se_3$ with targeted compositions $0.2 \leq x \leq 1.0$, were synthesised by placing the appropriate stoichiometric quantities of Li metal (Sigma Aldrich; 99%) and Bi_2Se_3 in a Schlenk tube with a magnetic stirrer bar. The Schlenk tube and a cylinder of ammonia (NH_3: BOC; 99.98 %, or ND_3: Sigma Aldrich; 99% D) were attached to a Schlenk line. After evacuating all pipework between the ammonia cylinder and the sample space, the Schlenk tube was placed in a slush bath of dry ice and isopropanol (-78 °C) to allow condensation of ammonia onto the reactants. For 0.40 g of Bi_2Se_3, around 15 mL of ammonia was condensed into the Schlenk tube. The solution was observed to briefly turn blue, characteristic of solvated electrons, after which the solution decoloured. The Schlenk tube was allowed to warm with the slush bath to room temperature over the course of around 4 h while boiling off ammonia [safety note: ammonia is volatile and toxic. Therefore, the Schlenk line was constructed so that any ammonia pressure could be relieved at all times via a mercury bubbler]. After evacuating the Schlenk tube, a dry dark grey powder was obtained.

Powder neutron diffraction

Powder neutron diffraction (PND) experiments were performed at 5 K and room temperature on the POLARIS diffractometer[1] at the ISIS Facility, Rutherford Appleton Laboratory, UK. Samples with NH_3 or ND_3 were contained in 6-mm-diameter thin-walled vanadium cans that were sealed with indium gaskets. Rietveld analysis was performed with TOPAS-Academic V5.[2]

In situ X-ray diffraction

The synthesis of the ammonia-rich Li-intercalated Bi_2Se_3 were performed on the I12 beamline[3] at the Diamond Light Source (UK) in an experiment conceived to investigate the structural changes during the intercalation process *in situ* and identify possible intermediate phases. The set-up was similar to that described previously for the intercalates of FeSe.[4] In an argon-filled glovebox, 3.2 (0.461 mmol) mg of Li and a small magnetic stirrer bar were loaded into the bottom of a 18 mm o.d × 4 mm wall Pyrex ampules sealed with high pressure Rotaflow Teflon valve [safety note: since these ampules were to be sealed with liquid ammonia at room temperature or below, they were professionally constructed and tested to withstand a pressure of 15 bar]. A stoichiometric amount of freshly synthesized Bi_2Se_3 (0.30 g, 0.461 mmol) was carefully placed into a side arm of the ampule to prevent direct contact with the Li. A Schlenk line setup was used to condense around 5 mL of ammonia onto the Li by placing the bottom of the ampule containing Li in a liquid nitrogen bath. On melting the ammonia ice in a -78 °C slush bath (mixture of dry ice and isopropanol), the Li fully dissolved and a blue solution characteristic of solvated electrons was obtained. The ampule was sealed and carefully transported to the beamline, with its bottom half in a bucket filled with slush, while maintaining the Bi_2Se_3 out of contact with the Li/NH_3 solution. The ampule was placed with the solution in the beam while clamped to a remote-controlled rotational stage and kept cool with a cold argon flow. While stirring the Li/NH_3 solution, diffractograms were measured upon exposure of the monochromatic 81.6 keV (λ = 0.15186 Å) X-ray beam and collected using a Pilatus CdTe 2M detector. Frames were collected continuously in time intervals of 100 ms separated by 400 ms dead time. To initiate the reaction, the ampule was rotated about the beam direction so that the Bi_2Se_3 poured out of the side-arm and into the solution. The evolution of the diffraction pattern was monitored for a few minutes to a few hours, depending on the reaction temperature used. Data reduction to integrate the diffraction pattern recorded on the 2D detector was performed using DAWN.[5] Data analysis of the powder data reduced to one dimension was performed with TOPAS-Academic V5.[2] Additional powder diffraction experiments on the intercalates, $Li_x(NH_2/NH_3)_yBi_2Se_3$, synthesised in-house with targeted compositions $0.2 \leq x \leq 1.0$ were performed on the I11 beamline[6] at the Diamond Light Source (UK) using 0.82 Å X-rays.

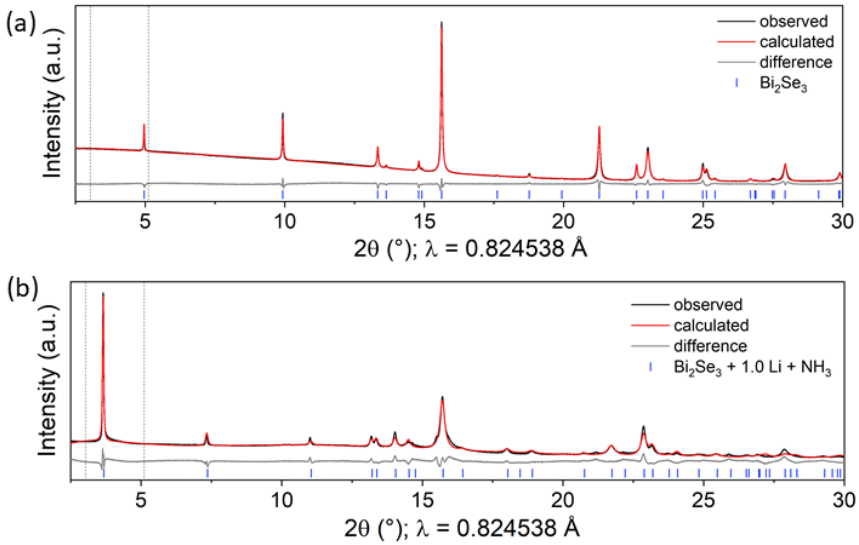

Fig. S1 Rietveld fits to I11 synchrotron data of Bi_2Se_3 and $Li_x(NH_2/NH_3)_yBi_2Se_3$ with $x = 1.0$, respectively. The dotted lines indicate the range plotted in Fig 1. The data in **(b)** is refined against Bi and Se positions only, as these heavy elements dominate the X-ray pattern (see main text).

Description of Rietveld refinements

A coupled Rietveld refinement for the highest resolution banks 3/8, 4/7 and 5/6 of the POLARIS diffractometers was performed on all four data sets in which a single structural model was used to fil all patterns. In this refinement, the lattice parameters for each data set were refined independently, to allow for small differences between the H- and D-containing samples and the changes in temperature, while the atomic positions and occupancies were coupled between each data set (*i.e.* the assumption was made that the structural model was temperature independents). Moreover, all atoms were refined with identical isotropic displacement parameters: one for the 5K data sets and one for the room temperature data sets. By assuming that substituting D for H does not impact the intercalations, and by benefitting from their different neutron scattering lengths, we forced the H and D occupancies to be the same in order to completely model the intercalated structure.

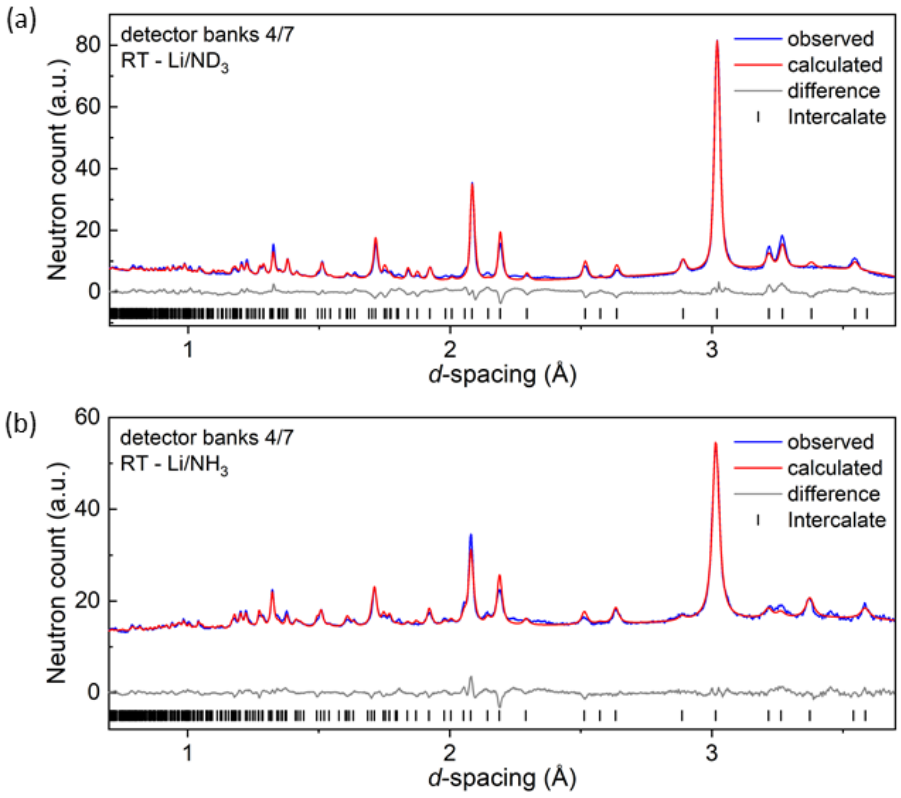

Fig. S2 Observed (blue) and calculated (red) powder neutron diffraction patterns and difference profile (grey) of the Rietveld refinements of the structure of the ammonia-poor **(a)** Li/ND_3 and **(b)** Li/NH_3 intercalates against POLARIS data at room temperature. Peak positions are marked by vertical lines.

Table S1. Structural and refinement parameters of POLARIS neutron diffraction data (esd's in parentheses).

Crystal Structure Data				
formula	$LiNX_2Bi_2Se_3$ (X = D/H)			
crystal system	hexagonal			
space group	*R*-3*m*:*H*			
formula units *Z* / cell	3			
temperature	5 K	5 K	room temperature	room temperature
ammonia	ND_3	NH_3	ND_3	NH_3
cell parameters / Å	*a* = 4.1484(4)	*a* = 4.1388(7)	*a* = 4.1657(5)	*a* = 4.1582(9)
	c = 38.136(4)	*c* = 38.092(7)	*c* = 38.598(5)	*c* = 38.585(9)
cell volume / $Å^3$	568.36 (13)	565.1(3)	580.06(16)	577.8(3)
Data collection				
diffractometer / radiation	POLARIS neutron diffractometer, time-of-flight measurement			
d-spacing range bank 1 / Å	0.94280 - 40.24778			
d-spacing range bank 2 / Å	0.66932 - 13.87116			
d-spacing range bank 3 / Å	0.32659 - 5.91452			
d-spacing range bank 4 / Å	0.20384 - 3.69421			
d-spacing range bank 5 / Å	0.14893 - 2.69895			
Structure Refinement				
method of refinement	Rietveld			
software	TOPAS-Academic V5			
r_wp refinement parameter	3.476			
Structure Parameters*				
Bi	x, y, z	0, 0, 0.28274(3)		
	multiplicity	6*c*		
	occupancy	1		
Se1	x, y, z	0, 0, 0.42272(3)		
	multiplicity	6*c*		
	occupancy	1		
Se2	x, y, z	0, 0, 0		
	multiplicity	3*a*		
	occupancy	1		
Li	x, y, z	1/3, 2/3, 0.50020(6)		
	multiplicity	6*c*		
	occupancy	0.5		

N1	x, y, z	1/3, 2/3, 0.50020(6)
	multiplicity	6*c*
	occupancy	0.5
X1	x, y, z	0.2510(8), -0.2510(8), 0.51942(11)
	multiplicity	18*h*
	occupancy	0.166(3)
X2	x, y, z	0.2512(6), -0.2512(6), 0.4844(3)
	multiplicity	18*h*
	occupancy	0.184(3)

*Refinement of atomic positions and occupancies were coupled for all four phases.

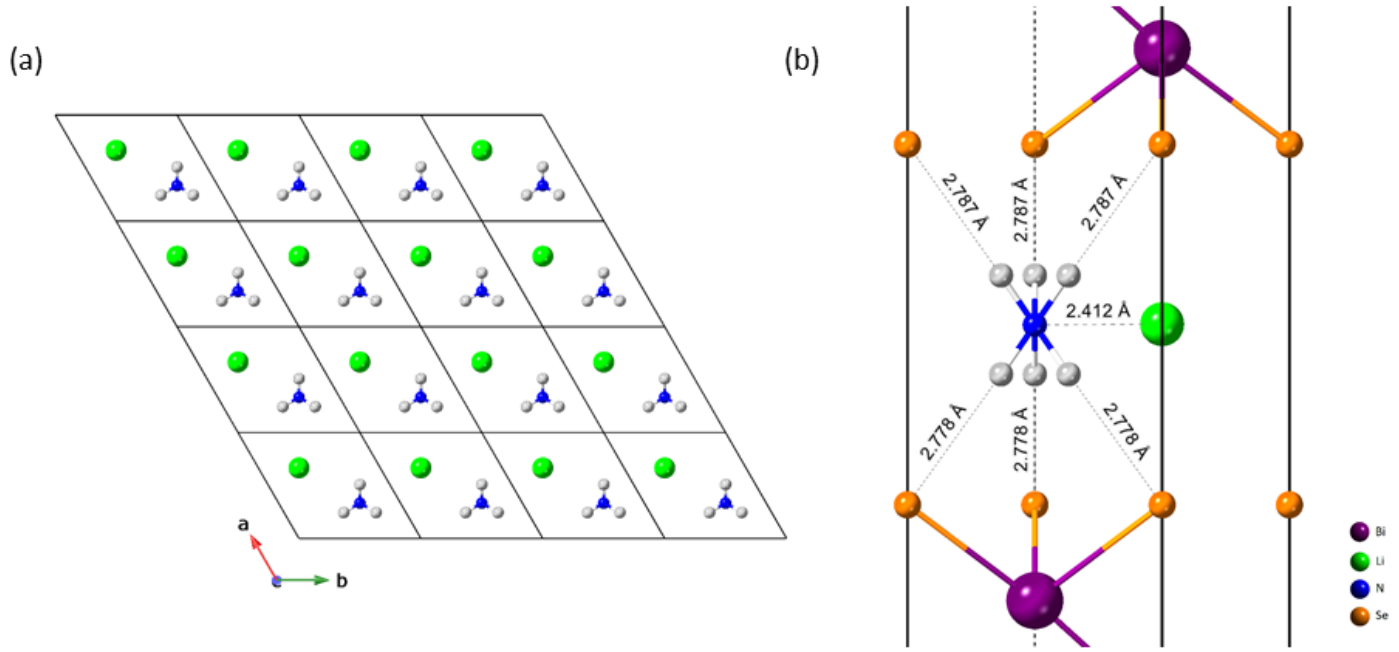

Fig. S3 (a) A single slab of Li and amide as intercalated in the van der Waals gap present in Bi_2Se_3, showing the honeycomb type lattice formed by the intercalates. In our model each layer is ordered, but there is stacking disorder of the intercalate layers leading to the average structure probed by diffraction having Li and NH_2^- moieties sharing a single crystallographic site. Note that the amide is orientationally disordered. **(b)** $LiNH_2Bi_2Se_3$ intercalate projected along the [210] direction, showing interatomic distances.

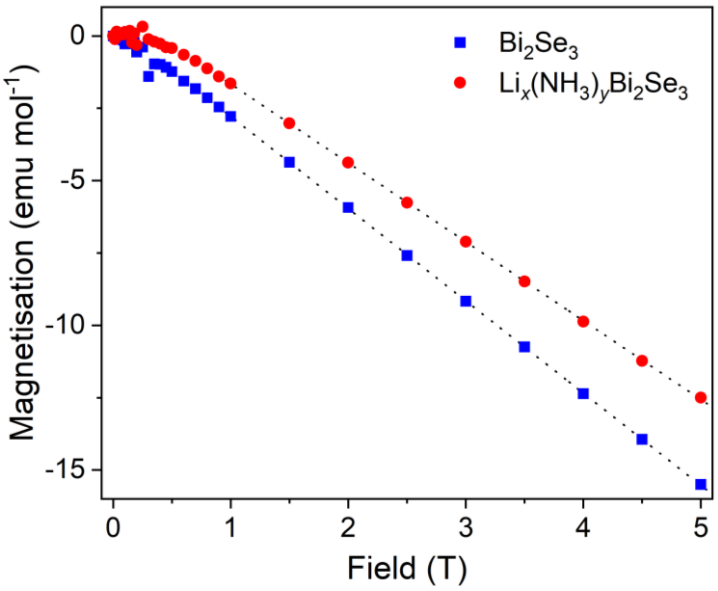

Fig. S4 *M* vs *H* for Bi_2Se_3 (blue) and its Li and ammonia intercalate (red) at 300 K. A magnetic impurity was evident at low fields but saturated above 0.5 T. The high-field linear fits (dashed lines) show that both phases are net diamagnets. Calculation of the magnetic susceptibility from the slope of the linear fits gives values of $-3.19(6) \cdot 10^{-4}$ and $-2.72(9) \cdot 10^{-4}$ for Bi_2Se_3 and its Li and ammonia intercalate, respectively.

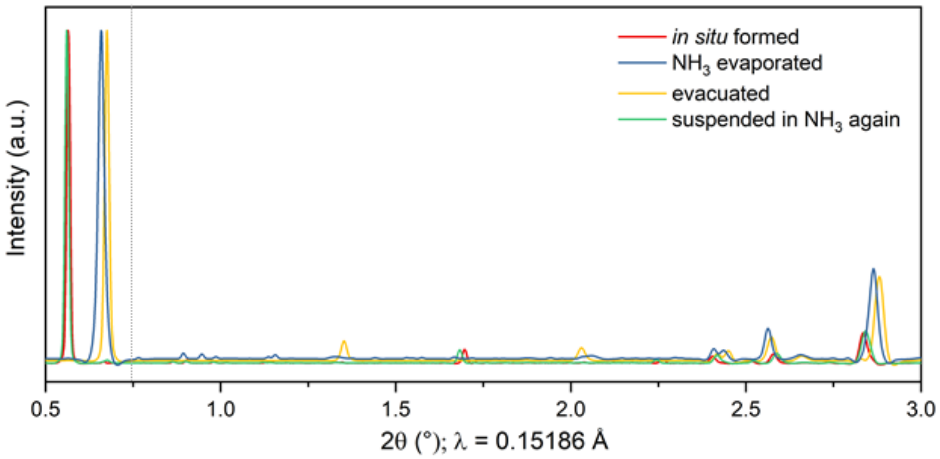

Fig. S5 PXRD pattern of the ammonia-rich intercalate as formed during the *in situ* reaction, after evaporation of NH_3, after evacuation, and after suspending again in liquid ammonia, showing the reversible nature of ammonia desorption as shown in Fig. 5. The background is subtracted for clarity. The dotted framework corresponds to the range plotted in Fig. 4. The lattice parameters of each structure is given in Table 1.

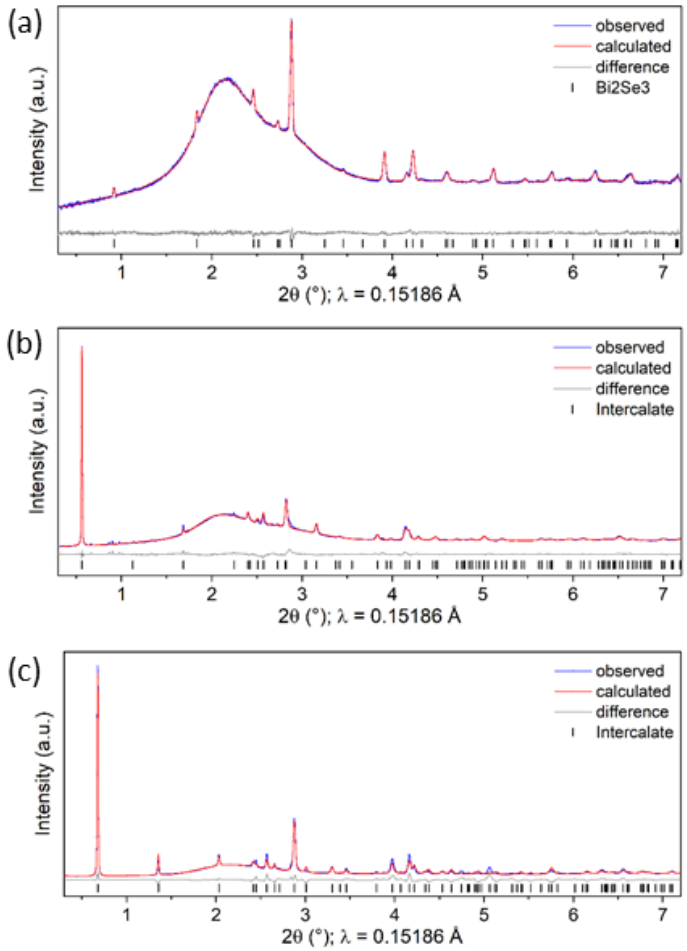

Fig. S6 Rietveld refinements against **(a)** the starting compound Bi_2Se_3, **(b)** the ammonia-rich intercalate phase and **(c)** the dried and evacuated final intercalate product, measured on the I12 beamline at the Diamond Light Source Ltd in the UK. Peak positions are marked by vertical lines. Corresponding schematic of crystal structures are given in Fig. 5.

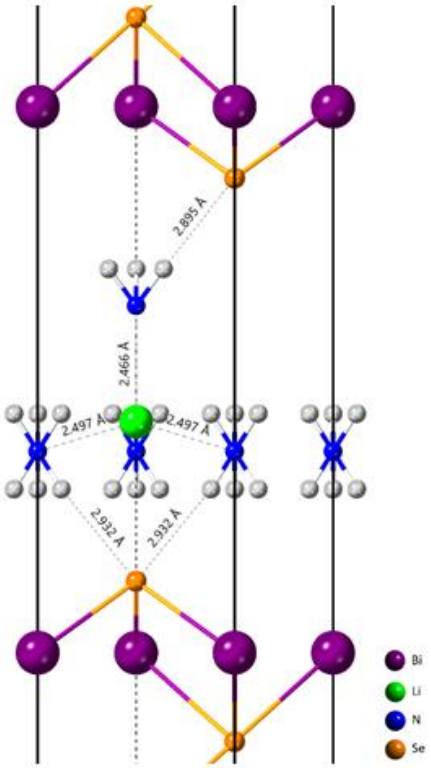

Fig. S7 Proposed model for the ammonia-rich intercalate projected along the [210] direction, showing interatomic distances.

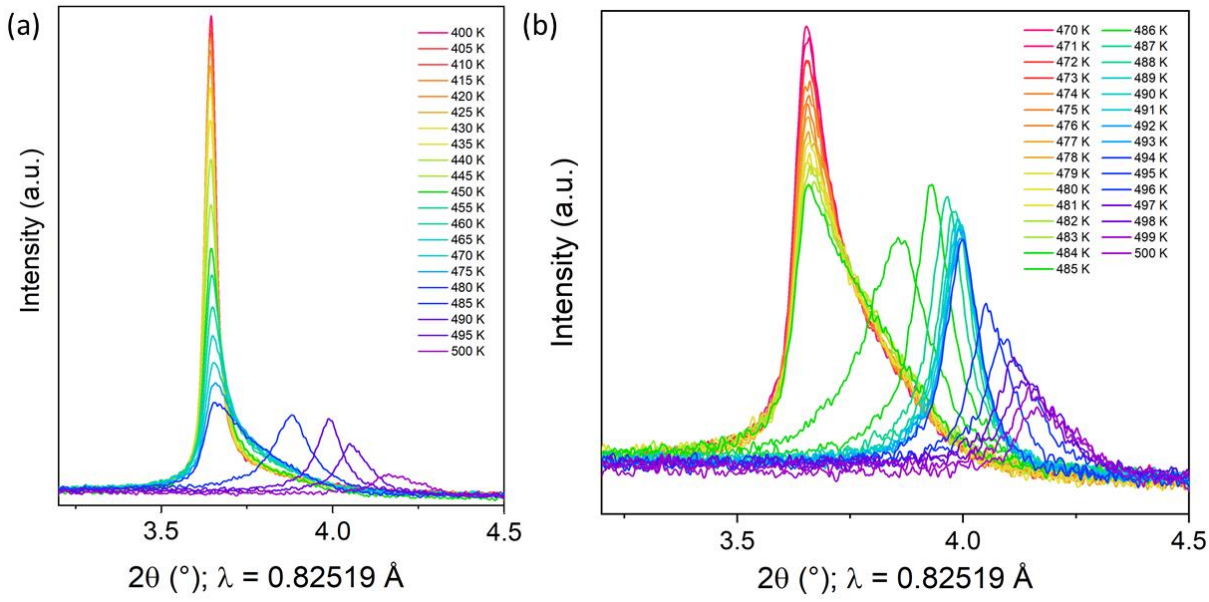

Fig. S8 (a) The 003 peak of $Li_2NH_2Bi_2Se_3$ as a function of temperature between 400 and 500 K, measured *in situ*. **(b)** The same 003 peak as a function of temperature between 470 and 500 K indicating the formation of an additional crystalline phase with a *d*-spacing of ~ 11.8 Å formed by annealing, prior to decomposition at elevated temperatures.

References

1 R. I. Smith, S. Hull, M. G. Tucker, H. Y. Playford, D. J. McPhail, S. P. Waller and S. T. Norberg, *Rev. Sci. Instrum.*, 2019, **90**, 115101.

2 A. A. Coelho, *J. Appl. Cryst.*, 2018, **51**, 210–218.

3 M. Drakopoulos, T. Connolley, C. Reinhard, R. Atwood, O. Magdysyuk, N. Vo, M. Hart, L. Connor, B. Humphreys, G. Howell, S. Davies, T. Hill, G. Wilkin, U. Pedersen, A. Foster, N. De Maio, M. Basham, F. Yuan and K. Wanelik, *J. Synchrotron Radiat.*, 2015, **22**, 828–838.

4 S. J. Sedlmaier, S. J. Cassidy, R. G. Morris, M. Drakopoulos, C. Reinhard, S. J. Moorhouse, D. O'Hare, P. Manuel, D. Khalyavin and S. J. Clarke, *J. Am. Chem. Soc.*, 2014, **136**, 630–633.

5 M. Basham, J. Filik, M. T. Wharmby, P. C. Y. Chang, B. El Kassaby, M. Gerring, J. Aishima, K. Levik, B. C. A. Pulford, I. Sikharulidze, D. Sneddon, M. Webber, S. S. Dhesi, F. Maccherozzi, O. Svensson, S. Brockhauser, G. Náray and A. W. Ashton, *J. Synchrotron Radiat.*, 2015, **22**, 853–858.

6 C. A. Murray, J. Potter, S. J. Day, A. R. Baker, S. P. Thompson, J. Kelly, C. G. Morris, S. Yang and C. C. Tang, *J. Appl. Cryst.*, 2017, **50**, 172–183.